Journal of Environment and Earth Science
ISSN 2224-3216 (Paper) ISSN 2225-0948 (Online)
Vol. 3, No.10, 2013
www.iiste.org

Petrology and geochemistry of Ourika gneissic rocks (High-Atlas, Morocco): Implications for provenance and geotectonic setting

Ahmed Barakat*, Jamila Rais, Mohamed El Baghdadi
Laboratory of Georessources and Environnement, Faculty of Sciences and Techniques, Sultan My Slimane University, P.O. Box 523, 23000 Beni-Mellal, Morocco
* E-mail of the corresponding author: a.barakat@usms.ma

Abstract

Gneissic terranes under studied are one of the various formations constituting the Ourika Old massif. They underwent a metamorphic evolution characterized by a first amphibole facies event and a second greenschist facies metamorphism. The high-grade metamorphism is related to a Pan-African orogenesis that produced subduction-related granitoids preserved as GAA and GBA gneisses. These two gneissic groups have different geochemical compositions which were likely linked to the protolith nature. Petrology and geochemical investigations reveal that the protolith of GBA gneisses is calc-alkali peraluminous S-type granodiorite and thus of GAA gneisses is calc-alkali metaluminous diorite. The GBA protolith showed a continental active margin characteristic that may belong to the earlier Pan-African event, at ~780 to 750 Ma, whereas the GAA protolith could be formed in the island arc/fore-arc event, at ~753 Ma. Both groups were ordered in two lines suggesting two different sources where the crustal intervention is more or less marked, by juvenile upper continental crust for GBA protolith, and by young lower continental crust for GAA protolith. Correlated to the anti-atlasic formations of the same age, the geochemical similarities suggest a comparable geodynamic evolution that is closely linked to a Neoproterozoic continental convergent margin in the north of West-African Craton (WAC), collided at late Pan-African orogenesis. This collision induced the strongly N-S deformation that was materialized by the overthrusting of the GAA protolith onto the GBA protolith, and by the forming of the Ourika gneissic massif as a submeridian dome.

Keywords: Ourika old massif; gneissic protoliths; Pan-African orogenesis; mineralogy and geochemistry; geodynamic evolution

1. Introduction

The Moroccan Precambrian terranes outcrop essentially in the south and more particularly in the Anti-Atlas (Figure 1a), as a very large inlier form. These terranes are attached to the West-African Craton (WAC), and constitute its western-northern edge. Their structuring is the result of the superimposition of various orogenetic phases from the Paleoproterozoic to the Paleozoic one.

The Precambrian basement of the High-Atlas is considered as the most septentrional termination of the Anti-Atlasic domain (Choubert and Marçais, 1952). It is surrounded by paleozoic and mezozoic formations and made up of Paleoproterozoic (PI) gneisses, of agmatites, schists and granodioritic rocks, quarzites and hornfels, volcanic rocks, and the pink granite intrusions (Choubert and Marçais 1952). Quarzites and hornfels were found in the Ourgouz and Taska-n-Zat series of Pre-Cambrian era (Lower and Middle Neoproterozoic) (PII), while the pink granite intrusions are of Upper Neoproterozoic (PIII). The volcanic rocks were found outcroping mainly in the Tircht massif (Choubert and Marçais, 1952).

The attribution of the Ourika gneissic rocks to PI age (Proust 1961; Choubert 1963; Leblanc 1981), was based on several characteristics such as, a very high degree of the metamorphism, a strong intensity of the deformation on the generally submeridian direction of the structural elements, and a lithological similarities with the PI rocks of the Anti-Atlas particularly those of the Bou-Azzer inlier. In previous studies (Juery *et al.*, 1974; Juery, 1976), the granodiorites and the pink granite, which constitute the major part of the outcrops of the old massif, were subjected to U-Pb and Rb-Sr radiometric datings. The estimated ages for the granodiorites and the pink granites were 610±15 Ma and 580±12 Ma respectively. In the same studies, Juery *et al.* (1974) tried to date the gneisses, but estimated a radiometric age largely posterior to that obtained for the granitoid ones, that was explained by the age rejuvenation related to the alteration of the gneisses. Thus, the Paleopoterozoic (2000 Ma) allotted to the gneissic rocks is always maintained.

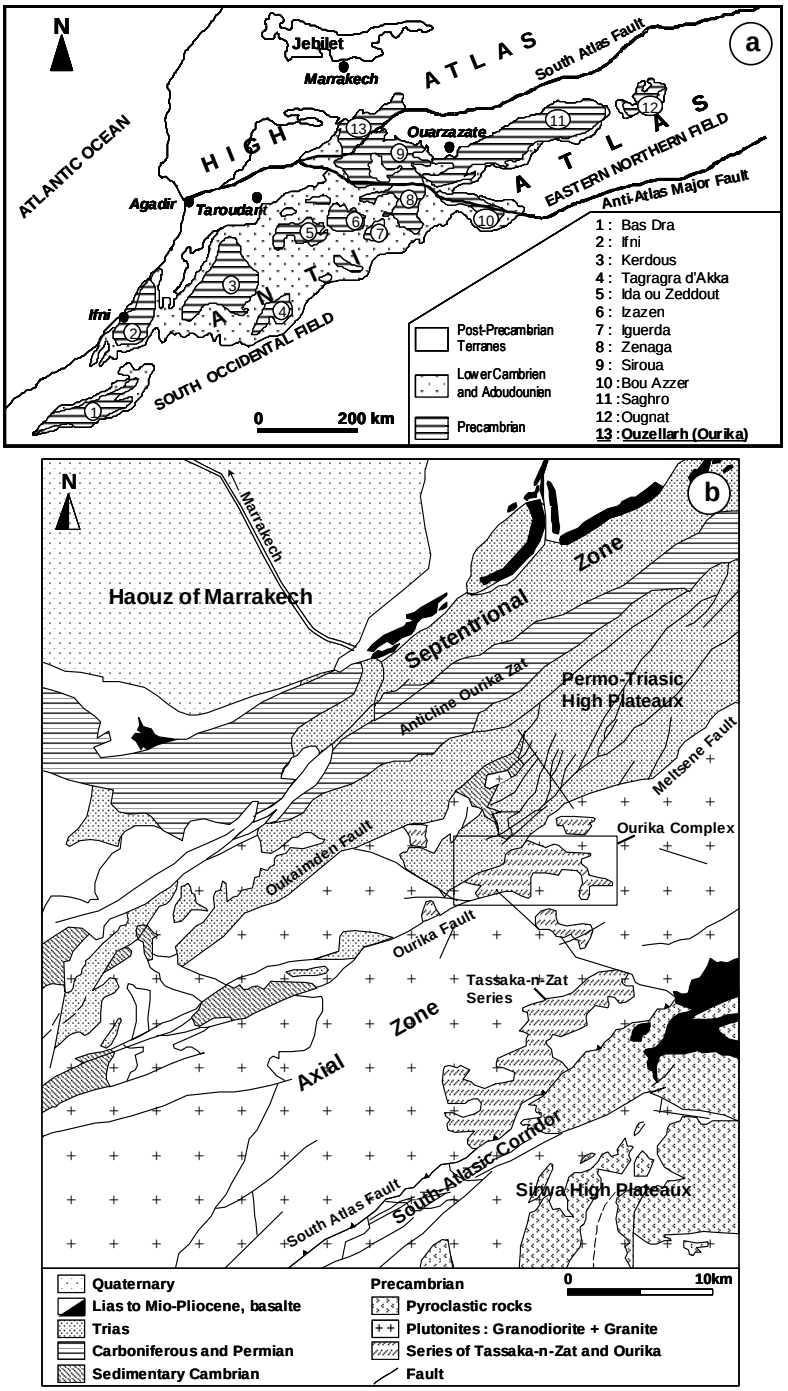

Figure 1. (a) Precambrian inliers of the Atlas regions (Choubert, 1963). (b) Structural map and subdivision of the Precambrian High Atlas massif (Vogel *et al.*, 1980)

Because of the nature of the sedimentological cycles, the metamorphism degree, and the correlations with the subdivision of Anti-Atlas Precambrian proposed by Choubert (1952), it was advanced that the Ourika gneissic massif of is made of different facies such as amphibolites, gneisses amphibolitic, migmatitic gneisses (Proust, 1961, 1973; Vogel *et al.*, 1980; Desutter, 1987; Raji, 1988; Nefly, 1998). The lithological and structural studies carried out by Nefly (1998) made it possible to interpret the gneissic massif in an elliptic diapiric dome with a submeridian direction. This author has subdivided this dome in a gneissic unit forming the core and an amphibolitic unit forming

the cover. The characterization of the protoliths (para-derived or ortho-derived) and the geodynamic evolution of these metamorphic units were the subject of few former studies (Proust, 1961, 1973; Desutter, 1987; Raji, 1988; Nefly, 1998) which were based mainly on petrography analyses that led to controversial results.

The present work corresponding to the petrology and geochemical study of the metamorphic rocks of the Ourika gneissic massif, was carried out. The obtained results were discussed and compared to the latest data on anti-atlasic rocks of the same age, referred to in the literature. This allowed us to characterize these metamorphic rocks and to get insight into their possible protoliths and geodynamic evolution.

2. Material and methods

2.1 Geological outline of the Ourika gneissic massif

The old basement of the Western High-Atlas belongs to the vast Ourika-Toubkal Precambrian inlier. It is subdivided in two geologically different blocks: a Western block composed of paleozoic formations, and an Eastern block formed of Precambrian crystalline (Neltner 1938; Proust 1973). This last block of the old basement is regarded as an advanced segment of the Precambrian central Anti-Atlas (Choubert and Marçais 1952). Following a correlation with the Siroua anti-atlasic massif, outcroping immediately in the south of the High-Atlas, it was called the "headland of Ouzellarh" by Choubert (1952, 1963) (Figure 1a). It is affected by major faults, generally oriented N70 °E (Nefly 1998). These directions are parallel to the direction of the Atlasic belt.

Figure 2. Geological map of the Ourika gneissic massif (Nefly, 1998)

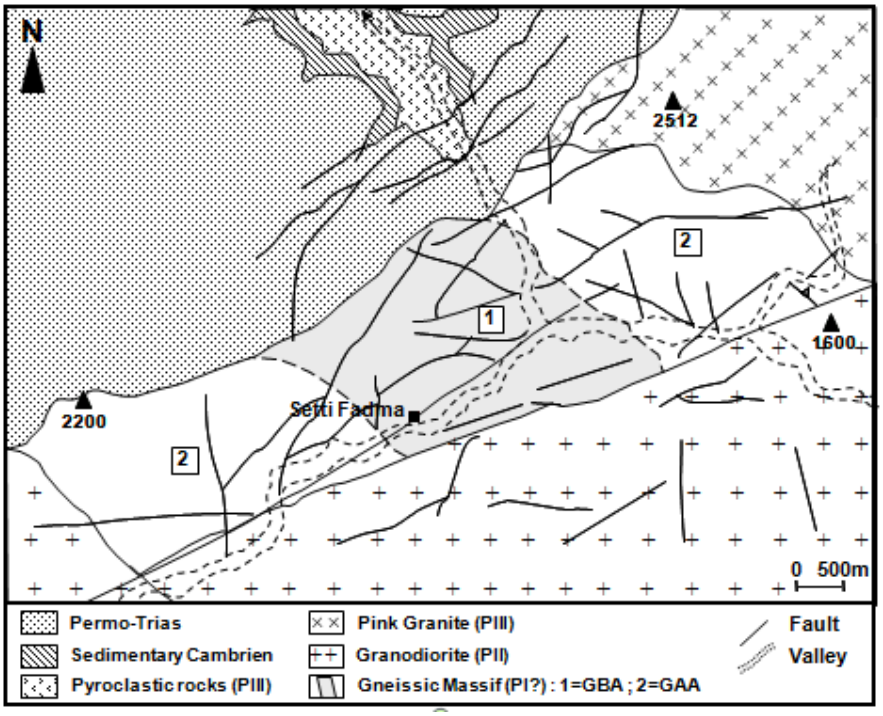

The gneissic massif of Ourika is located in the eastern bloc of the old basement of the High-Atlas, to approximately 60 km in the south of Marrakech (Figure 1b). The oldest formations of Precambrian era I (Proust, 1961, 1973; Leblanc, 1981; Vogel *et al.*, 1980) crop out at the Ourika river bend (Setti-Fadma village) (Figure 2). These formations constituting the gneissic massif appear as a depression, oriented N60 °E, of 5 km length and 2 km wide, and correspond to biotite-amphibole gneisses and amphibolites (Nefly, 1998). The gneissic massif is limited to the south and the west by granodiorites of PII age, to the east by pink granites of PIII age, and to north by triassic formations (Figure 2). These limits correspond to the Ourika and Melsem major faults respectivly to the south and to the north.

The deformation of the Ourika gneissic massif remains poorly knowned. This gneissic massif shows an important ductile deformation produced during the Precambrian orogenesis (Proust, 1961, 1973; Juery, 1976; Vogel *et al.*, 1980; Raji, 1988; Nefly, 1998). Two deformation phases were distinguished, corresponding to PI and PII Proterozoic (Raji,

1988). The PI deformation is characterized by an important foliation which affects the gneissic units. This foliation has a N130-160 °E and N30 °E directions, respectiveley in the east and west of the gneissic massif. It is expressed, at the scale of the sample, by an alternation of white and dark beds. This litage corresponds to an alignment of the biotite and amphibole crystals. The quartz grains showed a flatness associated with the early PI deformation. This latter express the effects of a syntectonic amphibolite-facies metamorphism, which is characterized by the appearance of the amphibole-biotite-quartz-oligoclase paragenesis. The PII deformation is due to a NNE-SSW compression, responsible for the development of the folds on various scales having an average N160 °E direction.

The brittle deformation, related to the episodes of post-PII deformation, is materialized by the development of a macro- and micro-structure system. These structures have mainly submeridian and subequatorial directions and other local directions. They are represented by faults, basic dykes and quartz filonnets (Barakat *et al.*, 2002a). These structures have a special importance because they played a structural control of the gold-bearing mineralisation of Ourika (Barakat *et al.*, 2002b).

For the petrological and geochemical investigation of the Ourika gneissic massif, different surface samples have been taken from two gneissic groups. The sampling and the study were conducted during the period 2002-2009.

2.2 Analysis

The petrologic and mineralogic characterization of the alteration and primary parageneses of both gneissic groups were carried out on various less altered samples taken in trenches and galleries of prospection. Mineral assemblages were studied using optical microscopy. Chemical composition of minerals (silicates and oxides) has been determined by electron microprobe (Cameca SX50 electron probe). Also, different samples from the GAA and GBA gneissic groups were analyzed for 10 major elements and 43 trace elements. Two techniques were used: ICP-AES for the major elements and ICP-MS for the trace elements. The result of the fusion in $LiBO_2$, was dissolved in HNO_3. The calibration was made by international geostandards.

3. Results

3.1 Petrography and mineral chemistry of gneissic rocks

The gneissic massif of Ourika appears as an elliptic dome of diapiric origin, with a submeridian direction (Nefly, 1998). Various facies, ± developed, were distinguished and gathered in two distinct and concordant groups. The first one in the center is formed by amphibole and biotite gneisses (GBA group). The other in the periphery consists of amphibolites and amphibole gneisses (GAA group) (Figure 2). These two groups and their minerals are described briefly in what follows.

3.1.1 Biotite and amphibole gneisses (GBA group)

Biotite and amphibole gneisses (GBA) could be divided into two facies: i) fine-grained gneisses, marked by the biotite abundance, showing by place a more or less important migmatitisation; ii) medium-grained gneisses, characterized by the abundance of amphibole, which were presented in the form of intrusion in the precedent facies. As a matter of fact, both faciès are very similar in their textures, structures, mineral composition and metamorphic grade, but are differing substantially by the size of crystals and the abundance of amphibole or biotite minerals. Both facies show an intense ductile plastic materialized by asymmetrical folds. They display fairly distinct foliation and mineral lineation marked by quartzo-feldspathic and biotite-amphibole beds. The mineralogical compositions observed in the two facies

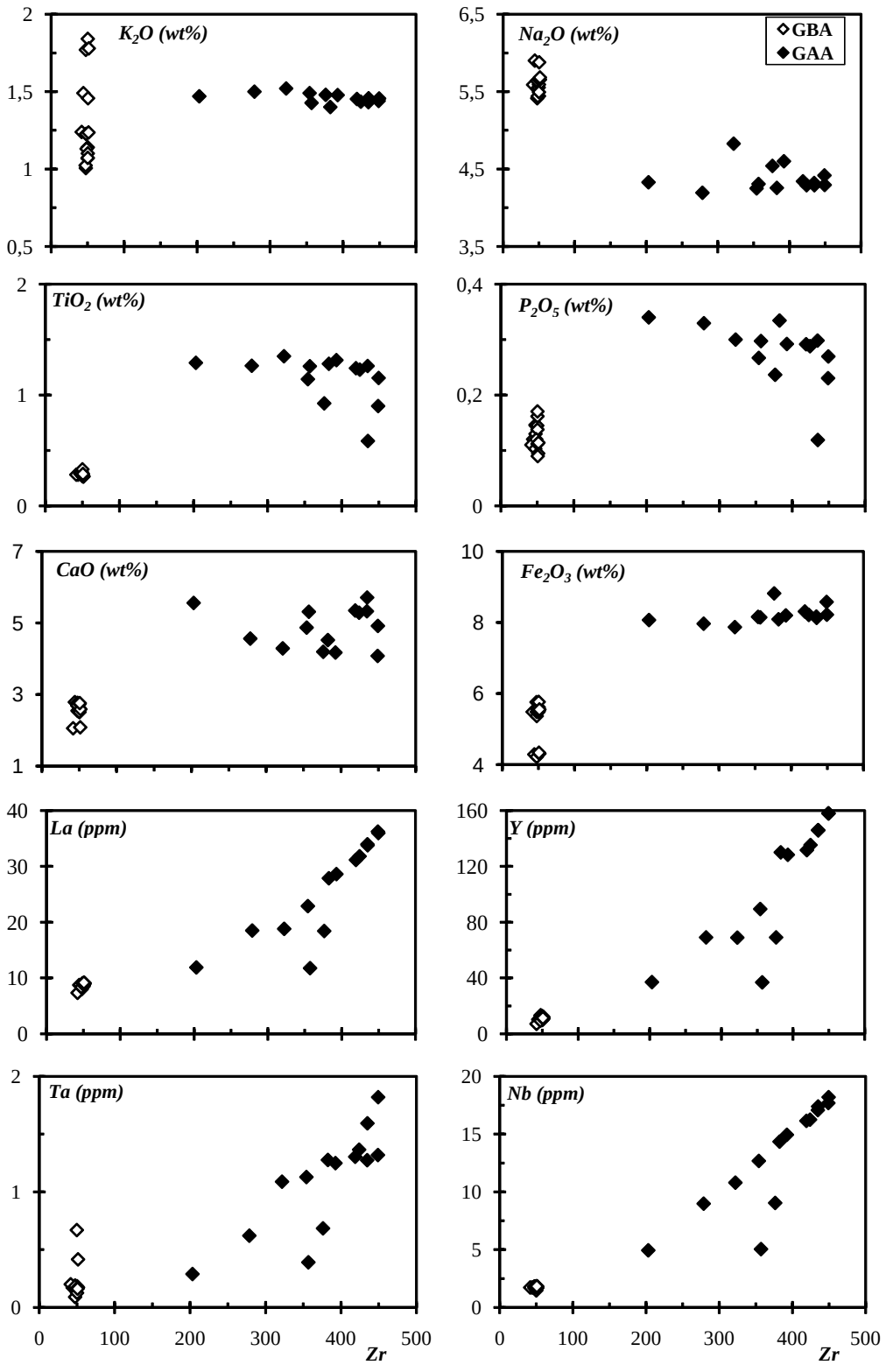

Figure 3. Selected major and trace element bivariante plots for the studied rocks using Zr as differentiation index

Table 1. Representative analyses of amphibole and plagioclase from Ourika metamorphic rocks. Ions calculated on the basis of : Amphibole, 23O and Fe* = Fe^{2+}; Plagioclase, 8O and Fe* = Fe^{3+}

	Amphibole									
	GBA group					GAA group				
	GT3/11	64	71	72	75	M4/11	M4/12	M4/b1	M4/24	MG/b1
FeO	14.66	14.5	15.75	15.96	15.5	16.28	16.58	16.61	16.57	16.51
Na_2O	0.3	0.4	0.83	0.38	0.66	1.29	1.37	1.32	1.08	1.49
K_2O	0.06	0.06	0.16	0.08	0.12	0.84	0.74	0.856	0.76	0.93
SiO_2	51.48	51.43	47.91	50.76	50.07	45.04	46.03	44.94	45.01	45.09
MnO	0.41	0.45	0.38	0.28	0.46	0.74	0.71	0.63	0.84	0.79
CaO	12.09	12.42	12.11	12.61	12.44	11.53	11.64	10.97	11.49	10.96
Al_2O_3	3.15	3.11	6.5	3.28	4.63	7.92	7.42	7.68	7.54	7.28
TiO_2	0,00	0.07	0.34	0.09	0.02	1.34	1.23	1.66	1.2	1.3
MgO	13.97	13.7	12.07	12.5	12.6	11.04	11.49	11.14	11.21	11.47
Total	96.2	96.3	96.18	96.07	96.65	96.12	97.31	96.01	96.03	96.05
Si	7.626	7.625	7.193	7.601	7.454	6.863	6.924	6.865	6.888	6.8979
Al tot	0.55	0.543	1.15	0.579	0.812	1.423	1.316	1.384	1.3606	1.313
Fe*	1.816	1.799	1.978	1.999	1.929	2.0752	2.086	2.123	2.121	2.112
Mg	3.085	3.027	2.701	2.789	2.795	2.506	2.576	2.535	2.558	2.615
Mn	0.052	0.057	0.049	0.036	0.058	0.096	0.091	0.082	0.108	0.103
Ca	1.92	1.974	1.948	2.022	1.984	1.883	1.875	1.795	1.884	1.796
Na	0.085	0.114	0.242	0.111	0.19	0.38	0.4	0.391	0.32	0.441
K	0.012	0.011	0.031	0.015	0.023	0.163	0.143	0.167	0.148	0.182
Ti	0,000	0.008	0.038	0.01	0.002	0.154	0.139	0.191	0.138	0.15
Al^{IV}	0.374	0.375	0.807	0.399	0.546	1.137	1.076	1.135	1.112	1.103
Al^{VI}	0.176	0.168	0.343	0.181	0.266	0.286	0.24	0.248	0.249	0.21

	Plagioclase							
	GBA group				GAA group			
	2	S11/1-6	FMIG/3-	GC/1-4	M4/b2	M4/b3	M4/21	M4/b4
FeO	0,00	0.09	0,00	0.1	0.11	0.17	0,00	0,00
Na_2O	11.7	10.71	11.72	11.54	9.32	9.55	10.84	7.59
K_2O	0.04	0.71	0.04	0.51	0.25	0.29	0.08	2.2
SiO_2	68.62	66.65	68.05	67.32	62.73	63.36	67.31	61.86
MnO	0,00	0.15	0,00	0,00	0,00	0.05	0.04	0,00
CaO	0.47	0.6	0.52	0.4	4.24	4.12	1.33	4.8
Al_2O_3	19.28	20.82	19.71	19.96	22.86	22.88	20.9	23.05
TiO_2	0,00	0,00	0.01	0,00	0.01	0,00	0,00	0,00
MgO	0.01	0.02	0.03	0,00	0,00	0.02	0.02	0.02
Total	100.12	99.85	100.07	99.96	99.62	100.63	100.51	99.5
Si	2.996	2.932	2.976	2.959	2.792	2.795	2.932	2.774
Al tot	0.993	1.08	1.016	1.034	1.199	1.19	1.074	1.218
Fe*	0,000	0.003	0,000	0.004	0.004	0.006	0,000	0,000
Mg	0,000	0.001	0.002	0,000	0,000	0.001	0.001	0.001
Mn	0,000	0.006	0,000	0,000	0,000	0.002	0.001	0,000
Ca	0.022	0.028	0.024	0.019	0.202	0.195	0.062	0.231
Na	0.991	0.913	0.994	0.984	0.804	0.817	0.96	0.66
K	0.002	0.04	0.002	0.029	0.014	0.016	0.004	0.126
Ti	0,000	0,000	0,000	0,000	0,000	0,000	0,000	0,000

are similar, and are composed of biotite, amphibole, plagioclase, quartz with minor ilmenite, garnet and chlorite. Sporadic distribution of epidote, apatite, sphene and sulfide was noticed.

Plagioclase blasts, very abundant, are completely or partially surrounded by amphibole crystals. They are partly replaced by sericite and chlorite. The plagioclase minerals which seem preserved, have often albite composition (An_1 to An_{11}) and seldom anorthite composition (An_{95} à An_{99}) (Table 1). The K-feldspars observed as small automorphic crystals, slightly represented, have a microcline composition. These feldspar types form beds with quartz which are found as coarse-grains and as small interstitial xenomorphic grains.

Amphibole, often associated to the biotite, appear as blades lengthened along schistosity plans. According to the classification of Leake (1997), the amphibole has a composition mainly of magnesian actinolite, and sometimes of magnesian hornblende (Table 1). Pressures of amphibole forming, estimated from the geobarometers of Brown (1977) and of Schmidt (1992), do not exceed 300 MPa, which corresponds to low depths (<10 km). Using the equation of Otten (1984) proposed for basaltic liquids, the estimated temperatures are about 540-600 ℃. Such temperatures correspond to greenschists-facies metamorphism.

Biotite, with a variable distribution and abundance, is presented as slats generally altered of chlorite. This chloritisation is accompanied by the sulphide formation. Biotite and amphibole form beds, intercalated with the quartzo-feldspathic beds.

The accessory minerals are represented by garnet, oxides (ilmenite) and apatite. Rare garnet crystals are often cracked and transformed into chlorite. Apatite, less abundant, is observed as inclusions. Ilmenite exists as small prismatic crystals associated to chlorite. Ore minerals include arsenopyrite, pyrite and chalcopyrite and are scattered in whole rocks.

3.1.2 Amphibolites and amphibole gneisses (GAA group)

The amphibolite and amphibole gneisses (GAA group) make a gradual continuation with the GBA gneisses. Their intense deformation is marked by the development of the amphibole beds and the quartzo-feldspathic beds. Mineralogical asssociation is composed of amphibole, plagioclase, quartz, apatite and ilmenite in varying proportions. Chlorite, epidote, sphene and Fe-sulfide are also found.

Amphibole, an abundant mineral, is presented as squat and directed crystals showing variable deformation. It presents a composition of magnesian hornblende, and seldom of actinolite composition (Table 1). Temperatures estimated from the amphibole composition are about 650-760 ℃ at 330±75 MPa, values corresponding to the amphibolite-facies metamorphism.

Subhedral plagioclase crystals are more or less sericitized. They yield andesine-oligoclase composition (Or_{36} à Or_{20}) (Table 1). Quartz is found in low quantity as small crystals. The accessory minerals are represented by apatite and ilmenite.

Secondary paragenesis (cholrite, epidote, sphene, etc), developed in both gneissic groups, are most often ascribed to retrogressive changes due to the posterior deformation and retrograde metamorphism. Chlorite results from the transformation of biotite, amphibole and garnet, and presents brunsvigite composition (diagram of Foster, 1962). White-micas, developped on various feldspars, give a phengitic composition. Small sphene crystals are generally present in cleavages of principal minerals. Epidotes (chemical formula) often developped into costs of plagioclase and amphibole minerals. They are also found, with chlorites and calcite, filling the veins. The sulphides are generaly represented by pyrite and arsenopyrite crystals that are disseminated in the gneisses.

3.2 Geochemistry of gneissic rocks

Trace and major elements data for analyzed samples (Table 2), were plotted in various chemical and mineralogical diagrams in order to determine the geochemical characteristics of both gneissic types.

The GAA group samples present the following average contents: SiO2: 58.74 wt%, Al_2O_3: 14.23 wt%, Fe_2O_3: 8,18 wt%, in MgO: 4.88 wt%, CaO: 4.45 wt% and alkaline elements : 5,84 wt%. In the GBA group, the average contents are : SiO_2: 62.43 wt%, Al_2O_3: 17.57 wt%, Fe_2O_3: 5.23 wt%, MgO: 2.58 wt% and CaO: 2.31 wt%. This group is slightly rich in alkaline (≈6.91 wt%) than the GAA. The trace element compositions of the two groups are remarkably distinct, especially for Nb contents (GAA: 12.47 ppm, GBA: 1.69 ppm), Ni (77.95 ppm and 6.39 ppm respectively), Y (103.44 ppm and 11.01 ppm) and Zr (369.61 ppm and 47.82 ppm). The difference in the two group compositions would be related to the diversity of the protoliths which could be sedimentary, volcano-sedimentary, or igneous nature. This diversity appears well in a selection of petrographic and magmatic discriminating diagrams. According to the normative classification, these two gnessic groups are placed between quartzic diorites and the quartzic monzodiorites.

Table 2. Representative geochemical analyses of metamorphic rock from Ourika gneissic massif

	GBA group						GAA group					
	SGNS	SGT1	SGP	SGT11	SGT4	SGTh	Mm2	Mt1	Mt2	Mm1	Mm3	Mt31
wt.%												
SiO_2	62.55	62.64	62.32	63.17	64.18	63.96	57.61	58.57	58.9	58.97	59.11	58.93
Al_2O_3	17.56	18.01	17.74	16.98	16.28	16.43	15.63	14.08	14.39	13.88	13.83	14.34
Fe2O3	4.29	4.22	5.49	5.37	5.48	5.49	7.87	8.07	8.58	8.22	8.15	8.09
MnO	0.08	0.07	0.1	0.07	0.05	0.06	0.2	0.21	0.22	0.2	0.2	0.21
MgO	2.79	2.55	2.06	2.77	2.69	2.73	4.29	5.56	4.08	5.29	5.32	4.52
CaO	2.41	2.25	2.37	2.2	2.07	2.1	4.13	4.66	5.45	4.08	3.94	4.67
Na2O	5.9	5.58	5.59	5.41	5.54	5.55	4.83	4.33	4.42	4.29	4.31	4.26
K2O	1.49	1.77	1.24	1.23	1.01	1.07	1.52	1.47	1.44	1.44	1.43	1.4
TiO2	0.28	0.3	0.28	0.3	0.3	0.27	1.35	1.29	0.9	1.23	1.26	1.28
P2O5	0.12	0.13	0.11	0.14	0.15	0.1422	0.3	0.34	0.23	0.29	0.3	0.33
LOI	2.35	2.33	2.54	2.29	2.2	2.23	2.19	1.94	1.33	2.1	2.14	1.95
Total	99.82	99.85	99.84	99.94	99.95	100.03	99.92	100.52	99.94	99.98	99.98	99.99
p.p.m.												
Ba	311,00	353,00	378,00	440.07	353.75	332,00	460,00	325,00	519,00	522.61	324.75	493.11
Cr	14.6	19.2	11.3	15.9	19.7	14.5	132,00	373,00	172,00	317.64	372.9	216.92
Hf	1.31	1.32	1.23	1.31	0.82	0.56	8.29	5.05	11.7	10.94	5.55	9.95
Nb	1.73	1.79	1.73	1.72	1.69	1.48	10.8	4.95	17.7	16.25	5.05	14.36
Ni	6.6	8.8	5.9	7.51	8.05	6.1	71.9	96.8	56.1	90.85	97.55	75.61
Rb	39.9	44.2	27.2	46.32	44.7	40,00	35.1	36.1	26.5	37.73	36,00	36.38
Sr	251,00	334,00	304,00	314,00	334.75	251.25	421,00	278,00	363,00	438.48	277.75	414.26
Ta	0.17	0.19	0.2	0.16	0.09	0.67	1.09	0.29	1.32	1.37	0.39	1.28
Th	2.35	1.21	2.04	1.54	0.46	3.1	2.54	0.93	3.1	3.03	1.68	2.69
U	1.23	1.17	1.6	1.17	0.67	1.33	1.03	0.33	0.92	1.03	0.83	0.89
Y	10.3	13.1	7.25	11.21	13.35	10.05	68.9	37.1	158,00	135.3	36.975	130.04
Zr	44.1	47.6	41.7	47.65	47.5	49.82	322,00	203,00	449,00	424.27	356.96	382.56
La	8.75	8.02	7.37	8.48	8.27	8.5	18.8	11.9	36.2	31.82	11.775	27.85
Ce	18,00	15.2	13.5	16.72	15.325	17.25	53.1	30.3	92.5	83.24	29.55	72.08
Pr	2.14	1.87	1.6	1.96	1.37	1.39	8.48	4.54	14.2	12.8	5.04	12.36
Nd	8.16	7.27	6.59	8.109	7.37	8.66	40.8	20.4	97.8	83.35	19.9	68.24
Sm	1.86	1.89	1.27	1.958	2.14	1.985	10.8	5.46	20.9	18.47	5.335	15.65
Eu	0.525	0.565	0.423	0.54	0.465	0.275	3.14	1.33	4.23	4.13	2.43	3.65
Gd	1.76	2.02	1.24	1.74	1.27	1.26	11.5	5.63	24.1	20.84	6.38	20.04
Dy	1.53	1.94	0.943	1.65	1.815	1.78	11.7	5.46	28.2	23.99	5.585	20.23
Ho	0.311	0.46	0.224	0.4	.492719	0.436	2.4	1.24	5.9	5.02	1.14	4.1
Er	0.965	1.1	0.662	0.88	1.55	1.465	6.73	3.56	15.7	11.36	3.31	7.59
Yb	1.1	1.34	0.804	1.16	1.215	1.35	6.75	3.78	14.8	12.73	4.53	10.9
Lu	0.182	0.203	0.118	0.16	0.078	0.432	0.985	0.579	1.99	1.72	0.704	1.66

Harker-type diagrams, when using Zr as differentiation index, for major and trace elements, were employed in order to compare rock groups within the gneissic massif (Figure 3), and to explore the extent to which the original chemical signatures of the basaltic protoliths may have been altered by element mobility during metamorphism and secondary alteration processes. The striking aspect on Harker-type diagrams is the clear individualization of two groups. Harker diagrams show clear trends for most major and trace elements. TiO_2, P_2O_5, Fe_2O_3, Na_2O and K_2O exhibit limited data scatter and positive correlation with Zr in GBA samples, but they are clearly scattered and show slight negative correlation with Zr in GAA samples. CaO shows a data spread in GAA group, explained by the posterior destabilization of amphiboles. Ta, Nb, La and Y elements exhibit limited and more data scatter respectively in GBA and GAA samples, and increase with increasing Zr.

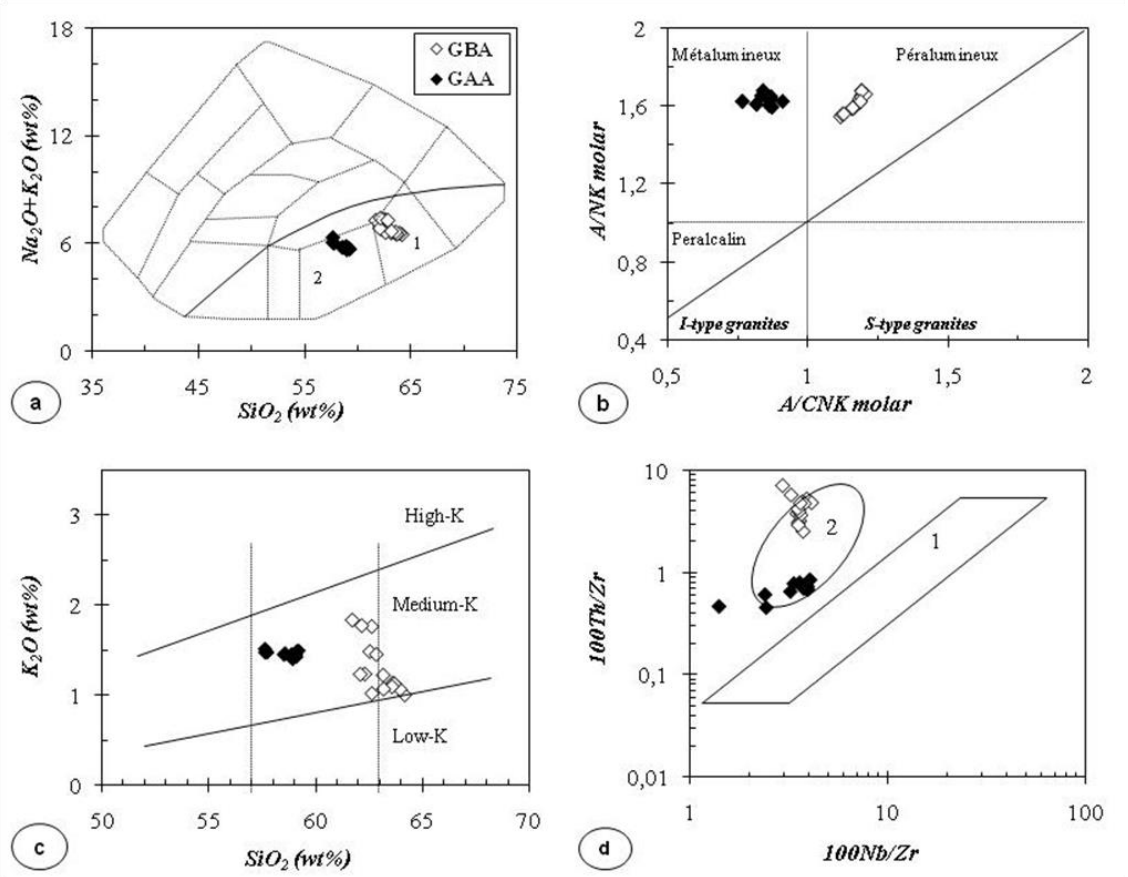

Figure 4. (a) Chemical classification diagram (Cox et *al.* 197; Wilson, 1989): 1, granodiorite; 2, diorite. (b) A/CNK vs. A/NK diagram [24]: A=Al2O3, C=CaO, N=Na2O, K=K2O (mol.%) ; (c) K2O vs. SiO2 bivariante diagram (Le Maitre, 1989). (c) 100Th/Zr vs. 100Nb/Zr (Beccaluva *et al.*, 1984): 1, Basic lavas no subduction setting; 2, basic and intermediate rocks with subduction setting

3.2.1 GBA gneissic group

The chemical classification and nomenclature of volcanic rocks using the total alkali (Na_2O+K_2O) versus SiO_2 diagram of Cox *et al.* (1979), adapted by Wilson (1989) for plutonic rocks, was used for the chemical classification and nomenclature of orthogneisses. On this diagram (Figure 4a) and in the Rb-Ba-Sr ternary diagram of El Bouseily and El Sokkary (1995), the GBA gneisses lie within the granodiorite or quartz diorite field and showed subalkaline affinity. Ti, Zr, Y and Nb elements, that are generally considered to be immobile during metamorphism (Winchester and Floyd 1977), showed comparable contents to those of the granodiorite or quartz diorite field. The Al_2O_3 and MgO values, according to Marc (1992), were similar to those of the orthogneisses. Plotted in A/NK versus A/CNK binary diagram (Shand, 1943) (Figure 4b), the

In the K_2O+Na_2O vs. SiO_2 diagram (Le Maitre, 1989), the samples displayed andesito-dacitic medium-K calc-alkaline (Figure 4c). On the AFM ternary diagram with the dividing lines of Jensen's (1976), the GBA rocks follow a calc-alkaline trend.

The REE spectrums (normalizing values from Sun and McDonough, 1989) of the GBA groups (Figure 5a) were clearly enriched in LREE (LaN/YbN: 4.29-6.58) and become clearly calc-alkaline, as proved by Jensen's (1976) diagram. There was no appreciable Eu-anomaly. The HREE and Y depletion could be explained by the presence of garnet in the melt.

The MORB-normalized spider diagrams for the incompatible major and trace elements showed a signature similar to that of subduction-related calk-alkaline basalts (Figure 5b). However, there was a clear enrichment of LIL elements Sr, K, Rb, Ba and Th with a characteristic Rb-peak, followed by a sharp drop of Ta and Nb. A relative enrichment for

La, Ce and Sm, as well as a variable fluctuation of Y and Yb, is marked. The subduction-related nature was also supported by other chemical ratios, as seen in the Nb/Zr vs Th/Zr diagram by Beccaluva et al (1984) (Figure 4d). The subduction signature is mainly due to the crustal contamination affecting the magmatism in a volcanic arc in both ocean arcs and continental margins. The calc-alkaline nature of the GBA protolith and the P to Yb content fluctuates around 1 confirming an origin in continental margin. The similarity between the normalized patterns of the GBA group and to those of the novate pot-collisional granitoids (Italian alps; Pearce *et al.*, 1984), and of the Java arc granites (Pearce *et al.*, 1984), interpret the GBA protolith as subduction-related magmatic-arc or post-collision-related complex.

The multi-element diagram has a steeper slope and was richer in LIL elements and lower in Sr, P, feature similar to that of sedimentary materials. TiO_2 Content falls between 0.27% and 0.30%, comparable to continental island-arc sediments (Bhatia, 1983). The low TiO_2 values of the samples are comparable to upper crustal values (Taylor and McLennan, 1985; Wedepohl, 1995) and are likely due to the general Ti depletion in arc environments.

3.2.2 GAA gneissic group

The GAA group of metamorphic rocks is placed in the field of the metaluminous I-type igneous rocks, attesting an ortho-derived origin (Figure 4b). On the (Na_2O+K_2O) versus SiO_2 diagram, the GBA gneisses lie within the diorite field and show subalkaline affinity (Figure 4a). The calc-alkaline tendency, weakly potassic and andesitic is shown in the SiO_2 versus K_2O diagram (Figure 4c). However, it's clear Eu-anomaly which is identical to that of diorites of other localities in the world (Eu/Eu*=0.69), pleads for a dioritic chemical composition more than andesitic. The andesitic rocks do not show this relatively high fractionation of plagioclases and consequently have a Eu/Eu* ratio rarely lower than 1. Using the classification of Barbarin (1999), based on the mineralogy and he major element geochemistry, the GAA protoliths would be of metaluminous granitoid type with mixed origin (mantellic + crustal) related to subduction regime.

The GAA group spectrums, roughly parallel, display slighly LREE-enriched patterns [(La/Yb)N = 1.71-2.26], with REE global ranging between 95 and 363 ppm, and commonly a slight depletion in La and Ce (Figure 5a) that may be explained by the extraction of LREE-rich minerals such as apatite. This spectrum feature would represent not very evolved magmatic materials probably very close to the magmatic source. They present an apparent negative Eu anomaly [Eu/Eu*=0.58-0.86] which might be related to plagioclase fractionation. The uniform increase in global REE contents and the roughly parallel spectra may be the results of shallow magmatic differentiation.

In the N-MORB spiderm (Figure 5c), the GAA proup show LILE-enriched and HFSE-depleted patterns, characteristic of arc-derived rocks, and an enrichment in Y and Yb materializing the intervention of an intraplaque component. The slight content increasing from La to Ba is observed, with values always exceeding MORB abundances. Ti and P elements show important negative anomalies, and clear inverse correlations with Zr, what is explained by either a role of apatite and ilmenite minerals in fractional crystallization or their poor contents in GAA rocks or these minerals are strongly transformed under the tectono-metamorphic events that affected these terranes. LILE elements (Sr, K, Rb, Ba) are not scattered, suggesting that their compositions were not modified by a subsequent metamorphism, and that's why they have been used to charachterize the protolith of GAA group. A remarkable negative Ta-Nb anomaly and higher concentrations in most elements were characteristic of arc magmatism. Yet, the normalized spedigrams compared to reference granites (Pearce *et al.*, 1984), are placed between the within-plate Mull granite and the arc Java granite. This indicates an arc-related source but not necessarily an arc environment at the time of GAA protolith, i.e. that it is formed far from the arc. This is an argument that the GAA group would be related to a particular environment which is island arc to fore-arc basin environment.

4. Discussion

4.1 Petrogenesis

In order to interpret a possible petrogenical evolution of the GAA and GBA protolihs, various elements (Ce, Nb, Y, Cr, Th, Ta, Yb, Zr) have been used in order to identify the tectonic. The uniform increase in global REE contents may be the result of shallow magmatic differentiation. Therefore, the narrow variation of the (La/Yb)N values and according the TiO_2, Fe_2O_3 and MgO components for both groups indicate a generation by partial melting of rock source, at a depth relativly higher for GAA protolith (≈14 km) than for GBA protolith (≈10 km)

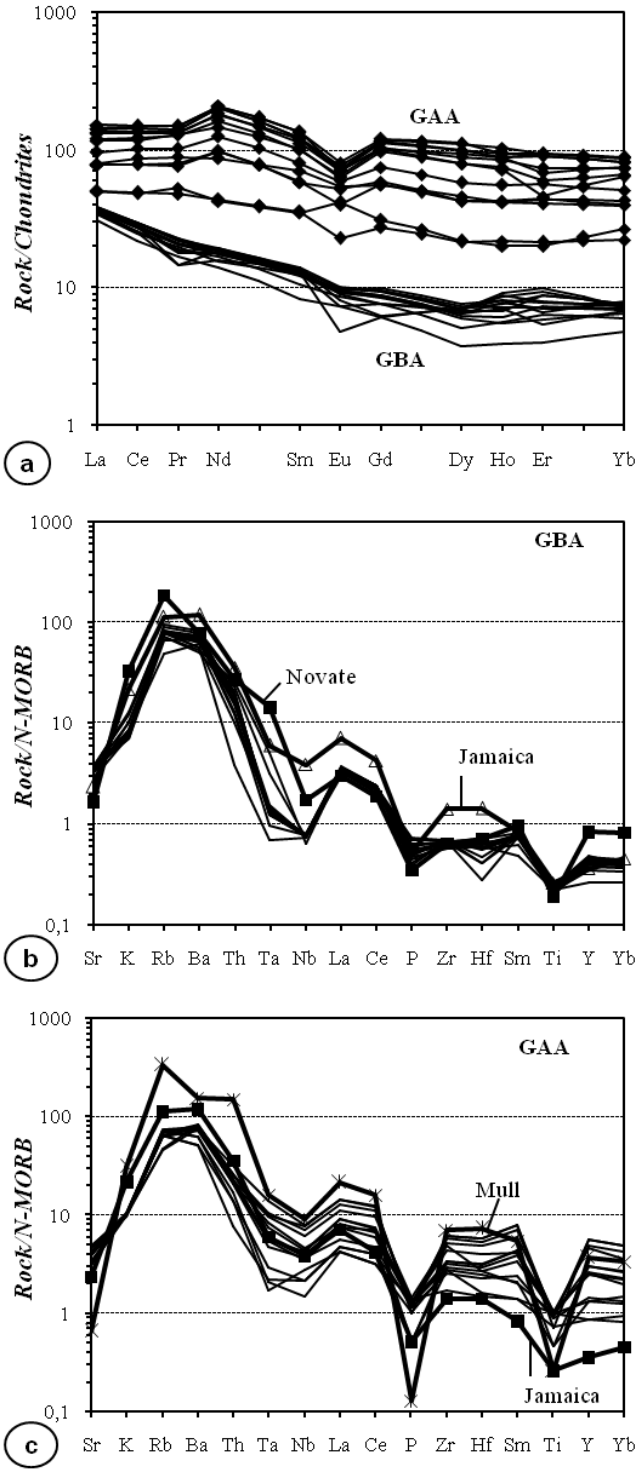

Figure 5. (a) Chondrite-normalized REE plot (normalizing values of Sun and McDonough, 1989) for GBA and GAA samples. (b) MORB-normalized plot (normalizing values of Sun and McDonough, 1989) for GBA samples. (c) MORB-normalized plot (normalizing values of Sun and McDonough; 1989) for GAA samples. Jamaica, Mull and Novate reference spectra from Pearce *et al.*, 1984

The positive slope in Ce/Yb versus Ce diagram (Figure 6a) displayed by GBA samples can be attribued to variable

degrees of partial melting from primary source. This source is far from being within-plaque or MORB type, as it was already shown before. Also, the absence, sometimes slightly, of Eu-anomaly in GBA group could exclude an origin from fractional crystallisation of primitive melts. Studies of felsic magmatism have confimed that melts from a garnet-bearing source are strongly depleted in HREE (Y<15ppm, Yb<1.4ppm) (Drummond and Defant, 1990). The GBA group were depleted in Y (7.25-13.35ppm) and Yb (0.8-1.35ppm); this suggests that the parental melt of the GBA protolith was derived from the garnet-bearing source resulting from melting of the continental crust than the mantle wedge. Also,the absence of apparent Eu anomalies could preclude an origin from fractional crystallisation of more primitive melts.

For GAA samples, the sub-horizontal tendency in Ce/Nb versus Ce diagram (Figure 6a) can be linked to the predominance of fractional crystallization. Significative Eu-anomalies showed in this group, are in agreement with a fractionation, that occured within the stability field of plagioclase. So, this GAA group displays a slight spread of Ce/Yb ratios reflecting minor differences in the degree of melting or source heterogeneity. These Cr and Y values are also very variable suggesting variable degrees of fractional crystallisation and lower degrees of melting (better lower than 3%). The high Y and Yb values suggest that the GAA protolith results from fractional crystallisation of a less evolved magma formed, in the absence of garnet, from the melting of mantle wedge than the continental crust. Also, the high Al and Mg percentages indicate that the magma-parent of the GAA protoliths would derive from a hydrated tholeitic source marked by the crystallization of Al and Mg-poor minerals (olivine and pyroxene) (Crawford, 1987; Debari and Sleep, 1991). Some authors considered that the magmas of the marginal basins, in equilibrium with the mantle at the top of the subducted-zone, are characterized by high Al contents (Marsh, 1986; Myers, 1988), which proves that the GAA protolith would form in a context of subduction-related basin.

Other informations on the source of the magmas are given by Yb/Nb, Zr/Nb, Th/Yb and Ta/Yb ratios that indicate an evolution to lower continental crust (LCC), dominated by fractional crysttallization with an intraplaque contamination, for the GAA group samples show, but the GBA group samples evolved to the upper continental crust (UCC) indicating that a more enrichment likely linked to the crustally contaminated continental margin arc.

4.2 Geodynamic outline

The magmatogenes of the subduction zones are marked by an enrichment in LILE elements and an impoverishment in Nb-Ta. The overall spectrum (Figure 5) of the GBA and GAA groups show the depletion of Ta and Nb relative to the LREE and the enrichments of LILE elements such as Ba, Rb and U relative to the HFSE or REE (Gill, 1981; Pearce, 1982; Hawkesworth *et al.*, 1993) wich are a characteristic of arc magmatic rocks. As seen in the Th-Zr diagram, all samples of both groups with their high Th/Zr ratio to be restricted within the range of subduction-related rocks.

On the Ta versus Yb tectonic-setting discrimination diagram (Figure 6b), all GBA samples occur in the arc field with an clear tendency from the collisional field, but these of GAA group show an advanced trend from MORB-WPG field to ARC field. Nevertheless, the patterns of GAA group, presenting a within-plate and ORG to arc affinities, demonstrate that there are a relative enrichment in large ion lithophile (LIL) elements (Rb, Sr and K) over the other incompatible elments (Nb, P, Zr, Ti and Y). This feature is commonly apparent in volcanic arc granites that are normally characterized by enrichiments in K, Rb, Ba, Th (typical in calc-alkaline rocks) and Ce relative to Nb, Zr an Y. TiO_2 values which are about 0.27-0.30% for GBA group, are comparable to upper crustal values, and about 0.59-1.35% for GAA group, are better comparable to lower crustal values to than MORB values. The clear Ti depletion seen in the two groups show also that they are quite related to an arc environments. The parent magma for the calc-alkaline series is a high-Al basalt (>14 wt% Al_2O_3), a type of basalt that is largely restricted to the subduction zone environment. The crustal contamination for both gneissic protoliths, described before, is also an agreement with a continental margin arc.

The La/10-Yb/15-Nb/8 (Pearce, 1982) and the Ta/Yb vs. Th/Yb diagrams (Cabanis and Lécolle, 1989) constitute a good summary (Figs. 6c, 6d): The GBA protolith shows the characters of a calc-alkalin basalt which is probably associated to an active continental margin; the GAA protolith indicates an intermediate characters with a more pronounced back-arc-basin signature.

The continental character of S-type granitoidic GBA protolith suggests a statigraphic within the uppermost part of continental segment, which melted in the context of a Pan-African orogenesis. This GBA protolith would be the result of the melting of the crustal or immature sedimentary rocks during the Pan-african continental margin. The GBA protolith formation in a late-orogenic context enabled him to escape from the Eburnean deformation and consequently from the associated metamorphism.

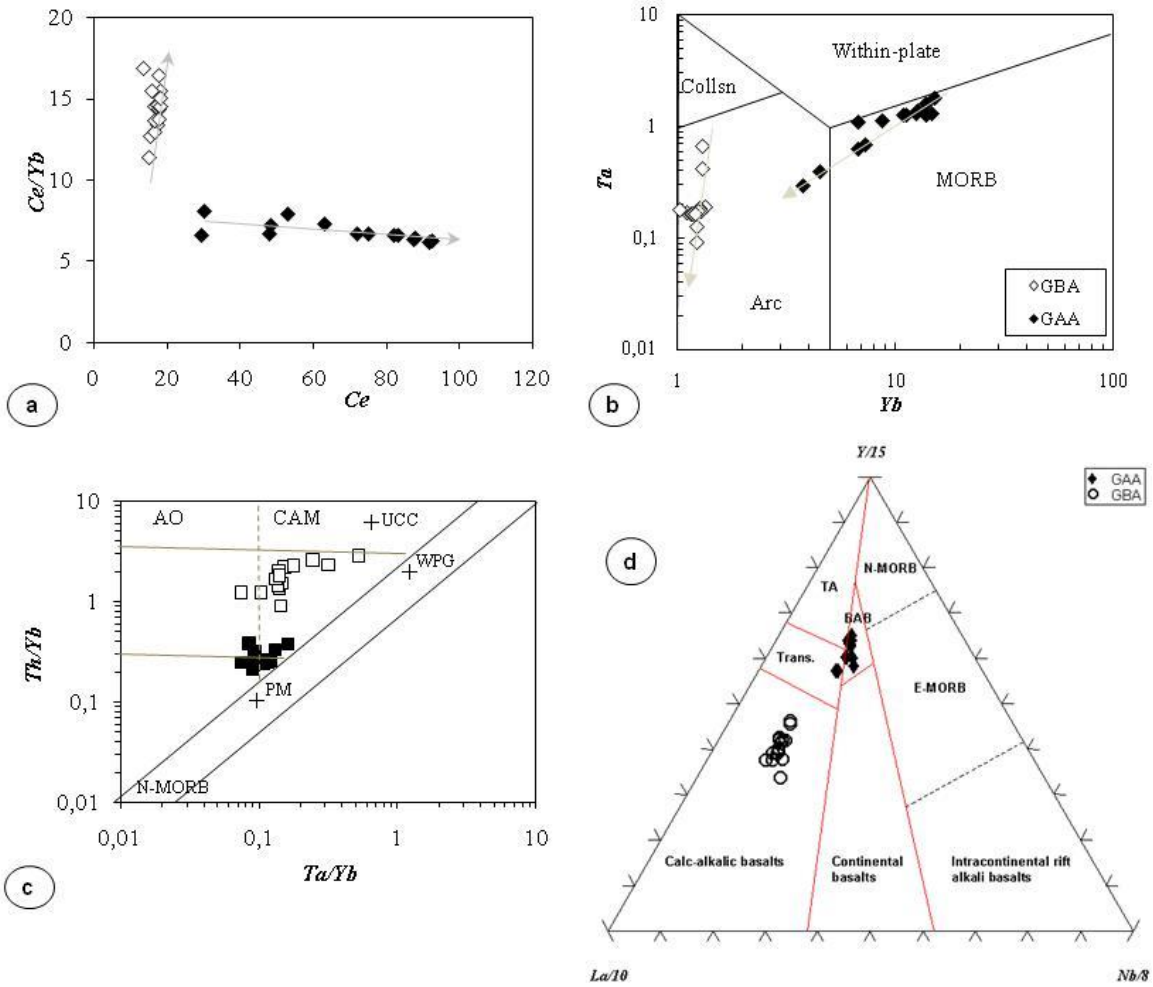

Figure 6. Petrogenical and tectonic-setting discrimination diagrams for the rocks studied. (a) Ce/Yb vs. Ce diagram (Gômez-Pugnaire *et al.*, 2003). (b) Ta vs. Yb diagram (Pearce, 1982); (c) Ta/Yb vs. Th/Yb diagram (Pearce, 1982). (d) La/10-Yb/15-Nb/8 triangular diagram (Cabanis and Lécolle, 1989); TA: Volcanic arc tholeiites; Trans: transitional; BAB: back-arc basalts

The intermediate geochemical characters of the GAA group would indicate that their genesis would be resulted of somewhat deeper fractionation of the primary tholeiitic magma which ponds at the base of the arc crust. Generally located under the subducted plate, this source appears only in certain cases such as near great fractures, subducted or crosscutting the arc (DeLong *et al.*, 1975) or near back-arc basins (Pearce, 1982). This and as seen in the La-Y-Nb diagram and the Nb-Ta anomalies and the intermediate position between a oceanic arc and a back-arc, attest likely that the GAA protolith by their transitional geochemical characters described before, would be related to island arc to arc basin. Compared to the similar Pan-African rocks of the Anti-Atlas, the GAA can be correlated with amphibolites of Bouazzer and with island-arc-related migmatites of Sirwa dated around 743 Ma (Thomas *et al.*, 2002).

From this geochemical compilation of the Ourika metamorphic rocks which reveals some information gaps (age-datings), it is difficult to elaborate a precise geodynamic model for them. Nevertheless, a signature of the arc/continental active margin type is clearly identified for the GAA and GBA gneissic protoliths whose forming

appears coherent with the model of subduction admitted for the Pan-African evolution of the Anti-Atlasic inliers. By comparison with the various geodynamic models advanced for the Anti-Atlas, in particular those proposed for Sirwa (Brabers and Vogel, 1985; Brabers, 1988; Thomas *et al.*, 2002, Thomas *et al.*, 2004) whose Ourika constitutes the northern prolongation, and for Bou Azzer (Saquaque, 1992; D'Lemos *et al.*, 2006) whose cores of the gneissic domes like to the GBA gneiss of the ourika, we can suggest the following geodynamic evolution in the Ourika old massif. This model proposes the opening and the closing of a marginal basin contemporary of a subduction below the septentrional edge of the WAC, during the Pan-African cycle. The marginal basin formation is contemporary with a northerly subduction under the detached micro-continent, thus an island arc-fore-arc basin environment was developed. This subduction took place some part in north in the High-Atlas (Brabers and Vogel, 1985; Brabers, 1988; Thomas *et al.*, 2002). It is accompanied by the magmatic events in the anti-atlas and by the formation of the Ourika GBA and GAA protoliths.

The GBA presents a continental character whose its formation seems early and closely related to the continental active margin. It would correspond to a platform facies resembling to the PIIa andesitic rocks described by Brabers and Vogel (1985) in the central Anti-Atlas, and to Tachakoucht rocks outcroping in the central part of Siroua inlier (Thomas *et al.*, 2002). These Tachakoucht rocks correspond to meta-andesite, reflecting the primary composition of the original rocks that have been explained as derivated products from mixtures of depleted mantle source and juvenile crustal material. Also, a further similarity between this GBA protolith and the Bou Azzer PI granite gneiss was described by Nefly (1998). These gneisses wrongfully considered of PI age in many previous works (Benyoucef, 1990; Saquaque, 1992), have been dated recently by D'Lemos *et al.* (2006) at *c.*753 Ma. Consequently, the GBA protolith identified before with PI would be more recent, of Neoproterozoic age.

The GAA protolith corresponds to an oceanic facies of the advanced phases of the expansion responsible for the insular arc formation. This let's suppose that the GAA prtolith is of lower-PII age, which in agreement with the Saquaque model which associated all amphibolites and ultrabasites supposed before of PI age, to the lower-PII formations. According to the Brabers classification (1988), these rocks would be attached to PIIb. Also, the GAA group shows a clear analogy with the migmatitic rocks of Iriri (Sirwa) dated to c. 743 Ma (Thomas *et al.*, 2002) and considered related to the island arc activity, which confirms the signature arc of the Ourika GAA protolith and their relatively recent age.

At some stage after, around 660 to 580 Ma (Thomas *et al.*, 2002), the closure of the marginal basin would have caused a collision between the island arc and the continent corresponding to the WAC. This bringing together was supported by one second southerly subduction. It was accompanied by tectono-metamorphic events responsibles for the important deformation of the ourika gneissic rocks, and of the overlapping of the GAA on the GBA protolith. The syn-collisional deformation is still marked by major thrusting, amphibolite to granulite-facies metamorphism and migmatisation by place. At this syn-tectonic deformation, is superimposed a pot-tectonic deformation which is marked much more in the intern zones (cores of the domes). This deformation has caused the folding of foliation, the appearance of the folds and a retrograde metamorphism in the green-schist facies. It is with this deformation that the diapiric activity was correlated (Nefly, 1998). Thus, the Pan-African deformation shows a N-S convergence with a strong gradient, and is responsible for the structuring as the dome of the Ourika gneisses. It is responsible for a crust thickening in the north of WAC. This thickening would have caused in Ourika, the formation of the gneissic dome with a light core under a heavy overload (Nefly 1998). The core corresponding to the GBA gneisses srongly affected by this deformation which led to green-schist to amphibolite-facies metamorphism, would have go, by ascending movements convectifs, in the heavy cover formed by the GAA gneiss. Pan-African late magmatism in Ourika is represented by the PII post-collisional granodiorite and the PIII pink granite.

5. Conclusion

The gneissic massif of Ourika is appeared as an elliptic dome of diapiric origin, with a submeridian direction. It is composed by various facies that gather in two distinct and concordant groups: amphibole and biotite gneisses (GAA) in center and amphibolites and amphibole gneisses (GAA) in periphery. The difference in the two group compositions would be related to the diversity of the protoliths. These latters underwent a tectonometamorphic evolution during the Pan-African orogenesis. The petrography and geochemical studies made it possible to have some informations on origin and tectonic significance of the GAA an GBA gneisses.

i) The protoliths of both gneissic groups represent a medium-K calc-alkaline from a subduction-related origin. They were peraluminous and S-type granitoids for GBA and metaluminous I-type diorites for GAA gneisses.

ii) The GBA and GAA protoliths that have until now been regarded as the PI terranes by many previous works, belong to a Pan-African orogeny, in which subduction, expansion and continental collision would have occurred to the northern edge of WAC. The GBA protholith seem to be generated by the melting of the crustal or immature sedimentary rocks after crustal thinning during the earlier Pan-African orogenic events, at 780 to 750 Ma compared to central anti-atlasic PIIa facies (Brabers and Vogel, 1985; Brabers, 1988) and Bou Azzer granite gneisses (D'Lemos *et al.*, 2006). GAA protolith were formed, more likely, in Pan-African island arc/fore-arc basin environments, from an anatexis related to the mantellic injection in the juvenile continental crust.
iii) The two gneissic protoliths have been affected by an amphibolite to granulite-facies metamorphism (700±50 °C) during the earlier Pan-African orogenic event and by a greenschist-facies metamorphism (570±30 °C), very developed in GBA protolith, during the late Pan-African orogeny.
iv) The strong N-S gradient of Pan-African deformation would be thus responsible for the for the overlapping of the GBA on the GAA protolith as well as for the dome shape of the Ourika gneisses, by thickening of the crust in the north of WAC. The dome core corresponding to the GBA gneisses which has been strongly affected by this deformation, would have intruded, by upward convective movements, in the heavy cover formed by the GAA gneiss. The late effects of Pan-African orogeny are marked by development of PIII granitoidic and granitic intrusions predated respectively at 610±15 Ma and 580±12Ma.

References

Barakat A., Marignac C., & Bouabdelli, M. (2002a). Les dykes basiques du massif ancien de l'Ourika (Atlas de Marrakech, Maroc): géochimie et signification. Caractérisation des minéralisations aurifères encaissées dans les gneiss précambriens de l'Ourika. *C. R. Géosciences*, 334: 827-833.
Barakat A, (2002b). Métallogénie des veines aurifères de l'Ourika (Haut-Atlas) et de Bleida (Anti-Atlas) : contrôles hydrothermal et structural. Thesis, Cadi Ayyad University, Semlalia, Marrakech, Morocco.
Barbarin B., (1999). The origin of granites and related rocks. Fourth Hutton Symposium abstracts, Documents du BRGM, 290: 1-249.
Beccaluva L., Dicorolamo P., Macciotta G., & Morra V., (1984). Magma affinities and fractionation trends in ophiolites. *Ofioliti*, 8(3): 307-324.
Benyoucef A., (1990). Etude pétrostructurale de la partie occidentale de la boutonnière de Bou Azzer - El Graara (Anti-Atlas), *Thèse 3ème cycle*. Université Cadi Ayyad, Marrakech, Morocco.
Bhatia M.R., (1983). Plate tectonics and geochemical composition of sandstones. *Journal of Geology*, 91: 611-627.
Brabers P., (1988). A plate tectonic model for the pan-african geology in the Anti-Atlas, Morocco. V.H. Jacobshagen (Ed.), *The Atlas System Of Morocco*, 6: 61-80.
Brabers P., & Vogel D.E., (1985). Modèle géodynamique de l'orogenèse panafricaine dans l'Anti-Atlas, Maroc. Proceeding of the 13th Colloquium of African Geology. St. Andrews, Scotland, Sep. 10-13, p. 19.
Brown E.H., (1977). The crossite content of Ca-amphibole as a guide to pressure metamorphism. *J. Petrol.*, 18(1): 53-72.
Cabanis B., & Lecolle M., (1989). Le diagramme La/10 –Y/15 –Nb/8: un outil pour la discrimination des series vocaniques et mise en évidence des processus de mélange et /ou de contamination crustale. *C.R. Acad. Sci. S.II*, 309: 2023-2029.
Choubert G., (1963). Histoire géologique du Précambrien de l'Anti-Atlas. *Not. Mém. Ser. Géol. Maroc*, 162: 1-352.
Choubert G., & Marçais J., (1952). Apperçu structural, in Géologie du Maroc. *Not. Mém. Ser. Géol. Maroc*, 100 fasc., 1: 53-71.
Choubert G., (1952). Essai d'application de la notion d'Infracambrien aux formations anciennes de l'Anti-Atlas. Proceeding of the 19th International Geological Congress. Alger, pp. 53-71.
Cox K.G., Bell J.D., & Pankhurst R.J., (1979). The interpretation of igneous rocks. George, *Allen and Unwin*, London, pp. 1-450.
Crawford A.J., Falloon T.J., & Eggins S., (1987). The origin of island arc high-alumina basalts. *Contrib. Mineral. Petrol.*, 97: 417-430.
D'Lemos R.S., Inglis J.D., & Samson S.D., (2006). A newly discovered orogenic event in Morocco: Neoproterozic ages for supposed Eburnean basement of the Bou Azzer inlier, Anti-Atlas Mountains. *Precambrian Res.*, 147: 65-78.
DeBari S.M, & Sleep N.H., (1991). High-Mg, low-Al bulk composition of the Talkeetna island arc, Alaska: Implications for primary magmas and the nature of arc crust. *Geol. Soc. Amer. Bull.*, 103: 37-47.

DeLong S.E., Hodges F.N., & Arculus R.J., (1975). Ultramafic nd mafic inclusions, Kanaga island, Alaska and the occurence of alkaline rocks in island arcs. *Journal Geology*, 83: 721-726.
Desutter F., (1987). Tendance de différenciation des amphibolites du massif ancien du Haut Atlas. *Mus. Roy. Afr. Centr.*, 84: 3137-3180.
Drummond M.S., & Defant M., (1990). Reply to comment by green and dawes on mount st. Helens : potential example of the artial melting of the subducted lithosphere in a volcanic arc. *Geology*, 22: 189-190.
El Bouseily A.M., & El Sokkary A.A., (1995). The relation between Rb, Ba and Sr in granitic rocks. *Chemical Geology*, 16: 207-219.
Foster M.D., (1962). Interpretation of the composition and a classification of the chlorites. *Us. Geol. Surv. Prof. Pap.*, 414A: 1-27.
Gill J.B., (1981). *Orogenic andesites and plate tectonics*. Springer Verlag, Berlin, p. 390.
Gomez-Pugnaire M.T., Azor A., Fernadez-soler J.M., & Lopez sanchez-Vizcaino V., (2003). The amphiboles from the Ossa-Morena/Central Iberian Variscan suture (Southwestern Iberian Massif): geochemistry and tectonic interpretation. *Lithos*, 68: 23-42.
Hawkesworth C.J., Gallagher K., Hergt J.M., & McDermott F., (1993). Trace element fractionation processes in the generation of island arc basalts. *Philosophical Transactions of the Royal Society of London*, A342! 179-191.
Jensen L.S., (1976). A new cation plot for classifying subalkalic volcanic rocks. Ontario Division Mines, *Miscelanea Paper*, 66: 1-21.
Juery A., (1976). Datation U-Pb du socle précambrien du Haut-Atlas (Maroc). Thèse 3ème cycle, Université Paris VII, France.
Juery A., Lancelot J.R., Hamet J., Proust F. , & Allegre C.J., (1974). L'âge des rhyolites du Précambrien III du Haut-Atlas et le problème de la limite Précambrien-Cambrien. Proceeding of 2ème réunion ann. Sci. Terre. Nancy, p. 230.
Le Maitre R.W., (1989). *A classification of igneous rocks and glossary of terms. Recommendations of International* Union of Geological sciences subcommision on systematics of igneous rocks, Blackwell, Oxford, p. 193.
Leake B.E., (1997). Nomenclature of amphiboles. *Mineral. Mag.*, 42: 533-563.
Leblanc M., (1981). Ophiolites précambriennes et gîtes arsénifés de colbalt (Bou Azzer). *Not. Mém. Ser. Géol. Maroc*, 280: 1-306.
Marc D., (1992). Granites and rhyolites from the northwestern USA: temporal variation in magmatic processes and relations to tectonic setting. *Transactions of the Edinburgh Royal Society, Earth Sciences*, 83: 51-64.
Marsh B.D., (1986). Principles of igneous petrology. *Amer. Jour. Sci.*, 286(7): 590-591.
Myers J.D., (1988). Possible petrogenetic relations between low and high MgO Aleutian basalts. *Geol. Soc. Amer. Bull.*, 100: 1040-1053.
Nefly M., (1998). Le massif cristallophyllien précambrien de l'Ourika (Haut Atlas de Marrakech, Maroc): Exemple d'un dôme gneissique d'origine diapirique. Thèse de Doctorat d'Etat, Université de Casablanca, Morocco.
Nelter L., (1938). Etudes géologiques dans le sud marocain (Haut Atlas et Anti-Atlas). *Not. Mém. Ser. Géol. Maroc*, 42: 1-298.
Otten M.T., (1984). The origine of brown hornblende in the Artssjället gabbro and dolerites. *Contrib. Mineral. Petrol.*, 86: 185-199.
Pearce J.A., (1982). *Trace elment characteristics of lavas from destructive plate*. Thorpe, R. S. (ed.), Andesites. New York: John Wiley and Sons, pp: 525-48.
Pearce J.A., Harris N.B.W., & Tindle A.G., (1984). Trace element discrimination diagrams for the tectonic interpretation of granitic rocks. *J. Petrol.*, 25: 956-983.
Proust F., (1961). Etude stratigraphique, pétrographique et structurale du bloc oriental du massif ancien du Haut Atlas (Maroc), Thesis, Université de Montpellier, France.
Proust F., (1973). Étude stratigraphique, pétrographique et structurale du bloc oriental du massif ancien du Haut Atlas (Maroc). *Not. Mém. Ser. Géol. Maroc*, 254: 15-53.
Raji M., (1988). Étude pétrographique et structurale du PI de setti Fatma (Haut-Atlas de Marrakech, Maroc), Thèse 3ème cycle, Université Cadi Ayyad, Semlalia, Morocco.
Saquaque A., (1992). Un exemple de suture-arc : le Précambrien de l'Anti-Atlas centro-oriental (Maroc), Thèse Doctorat d'Etat, Université Cadi Ayyad, Semlalia, Morocco.
Schmidt N.W., (1992). Amphibole composition in tonalite as a pressure : an experimental calibration of the Al in

hornblende barometer. *Contrib. Mineral. Petrol.*, 110: 304-310.
Shand S.J., (1943). *Eruptive Rocks: Their Genesis Composition, Classification, and their Relations to Ore Deposits*. John Wiley, New York.
Sun S.S., & McDonough W.F., (1989). *Chemical and isotopic systematics of oceanic basalts; implications for mantle composition and processes*. In Magmatism in the ocean basins. Saunders, A.D. and Norry, M.J. Ed., Geological Society of London, London, 42: 313-345.
Sylvester P.J., (1998). post-collisional strongly perluminous granites. *Lithos*, 45: 29-44.
Taylor S.R., & McLennan S.M., (1985). The continental crust : its composition and evolution Blackwell, Oxford. *Contrib. Mineral. Petrol.*, 100: 268-280.
Thomas R.J., Fekkak A., Ennih N., Errami E., Loughlin S.C., Gresse P.G., Chevallier L.P., & Liégeois J.P., (2004). A new lithostratigraphic framework for the Anti-Atlas Orogen, Morocco. *J. Afr. Earth Sci.*, 39: 217–226.
Thomas R.J., Chevallier L.P., Gresse P.G., Harmer R.E., Eglington B.M., Armstrong R.A., De Beer CH., Martini J.E.J., De Kock G.S., Macey P.H., & Ingram B.A., (2002). Precambrian evolution of the Sirwa Window, Anti-Atlas Orogen, Morocco. *Precambrian Res.*, 118: 1-57.
Vogel E.D., Missoten R., & Desutter F., (1980). Carte géologique du Maroc au 1/100000, feuille Oukaimden-Toubkal, Note explicative, KU Leuven, p: 131.
Wedepohl K.H., (1995). The composition of the continental crust. *Geochim. Cosmochim. Acta*, 59: 1217-1232.
Wilson M., (1989). *Igneous Petrogenesis*. Unwin Hyman, London, p: 1-466.
Winchester J.A., & Floyd P.A., (1977). Geochemical discrimination of different magmas series and their differentiation products using immobiles elements. *Chemical Geology*, 20: 325-343.